Nitrogen removal performance of microbial fuel cell enhanced bioretention system

Yajun Wang, Rajendra Prasad Singh **IWA**, Junyu Zhang **IWA**, Yan Xu and Dafang Fu **IWA**

ABSTRACT

Bioretention cell (BRC) and an enhanced system combining bioretention cell with microbial fuel cell (BRC-MFC) were used to treat domestic wastewater. Nitrogen removal characteristics and permeation characteristics of two systems were investigated by adjusting influent carbon/nitrogen ratio (C/N = 2–20). Results showed that nitrification and denitrification performances were mainly influenced by organic matter and system combination, which further effected the nitrogen removal. When optimal operating parameters were: electrode space of 30 cm, hydraulic load of 1.0 m^3/(m^2·d) and inlet/reaction time of 1/8 in BRC-MFC system, chemical oxygen demand (COD), total nitrogen (TN) and NH$_4^+$ removal efficiencies still reached 97.63, 64, and 42.26%, respectively and achieved high removal efficiency of organic matter and nitrogen simultaneously compared to the BRC system. Efficient supply of electron and phylogenetic diversity of bacterial communities in BRC-MFC process was the main reason to achieve deep denitrification removal. After the V3-V4 variable region of 16S rRNA gene was sequenced by the Miseq high-throughput sequencing method, introduction of MFC enhancement technology affected the microbial community structure in the system. The presence of MFC contributed to an increase in community diversity (from 14 to 19 phyla). The results provide a simple method without kinetic energy for simultaneous denitrification and steady infiltration of bioretention.

Key words | bioelectricity enhancement technology, bioretention cell, nitrogen removal, permeation characteristics, wastewater

Yajun Wang
School of Civil Engineering,
Lanzhou University of Technology,
Lanzhou 730050,
China

Yajun Wang
Rajendra Prasad Singh IWA
Junyu Zhang IWA
Yan Xu
Dafang Fu IWA (corresponding author)
School of Civil Engineering,
Southeast University,
Nanjing 210096, runon
China
and
Southeast University-Monash University Joint
  Research Centre for Future Cities,
Nanjing 210096,
China
E-mail: fdf@seu.edu.cn

INTRODUCTION

Media filtration is one of the oldest forms of treatment technology used in the production of potable water and it is still widely used due to its reliability and low cost. Bioretention (often referred to as biofiltration systems, biofilters, or rain-gardens) has demonstrated high removal of metals and suspended sediment from stormwater, while the reduction in nutrient concentrations displays greater variability (Payne *et al.* 2014a). However, the removal of stormwater pollutants is a relatively recent practice in situations that protect waterways. This includes nitrogen and pathogen treatment of stormwater for water reuse in water stressed areas (Payne *et al.* 2014a), or to meet the standards required for discharge into sensitive water courses and drinking water protected

areas (Zhou *et al.* 2017). Treating wastewater by bioretention is much more challenging than for stormwater due to the higher resources and energy required, much of which is organic in nature. To illustrate, the average influent nitrogen for a stormwater bioretention system is typically around 2.1 mg/L with occasional spikes up to 3.2 mg/L (Payne *et al.* 2014b). However, domestic effluents typically have total nitrogen between 40 and 50 mg/L which causes formidable loading in most conventional bioretention.

In China, the pollutant concentrations in municipal wastewater are lower in the south than in the north, especially the ratio of chemical oxygen demand to total nitrogen in influent (C/N ≤ 4–6). Therefore, it is extremely

difficult to achieve the efficient and stable removal of nitrogen in conventional biological treatment processes (Cao *et al.* 2013). A lack of electron donor is always the key limiting factor of nitrogen removal efficiency during denitrification process. New electrons or their donor are significant in nitrogen removal. The introduction of microbial fuel cell (MFC or 'biogeobattery') and catalytic iron has been recommended because it has demonstrated the capacity to enhance denitrification and thereby increase overall nitrogen removal. The biogeobattery phenomenon is caused by microbes driving the electron flow that is coupled to spatially separate biogeochemical processes. It is worth noting that some innovative hybrid systems were also reported recently based on the similarities in the design of constructed wetland integrated with biogeobattery for ensuring the efficiency of wastewater treatment and power generation. At the same time, a catalytic iron system has the advantages of high reduction ability, convenient in use, persistent in transporting electron and wide obtaining paths. Therefore, it has received significant attention in recent years.

In the classical biogeobattery model (Figure 1(a)), the conductor is a bacterial biofilm and/or conductive biominerals (e.g. magnetite, Fe_3O_4) straddling a redox gradient (e.g. the water table or the plume fringe), with the return current pathway through the surrounding pore fluid. The suggested mechanism is a microbial fuel cell (BRC-MFC) (Figure 1(b)), where organic matter at the anodic region was oxidized,

electrons (e^-) and protons (H^+) were produced and then moved to the cathode, with the return current pathway via insulated copper wires connecting the cathode and anode.

The study on bioretention and biogeobattery individually has been investigated on nitrogen removal extensively (Ge *et al.* 2019). However, the integration of bioretention and biogeobattery is still in its infancy, and it is highly likely to provide a promising technical path for improving the low nitrogen removal efficiency of bioretention. Hence, the study of biogeobattery integrated into bioretention is highly significant as it a promising technology to treat domestic wastewater with bioelectricity generation. In addition, to improve the understanding of the role of C/N ratio in nitrogen removal of bioretention coupling with biogeobattery treating sewage, all processes under natural conditions need to be studied. Therefore, in the present study, bioretention systems were operated to investigate the effect of influent different carbon nitrogen ratios and different combinations on nitrogen removal performance.

MATERIALS AND METHODS

Bioretention cell and microbial fuel cell assemble

Three bioretention (BRC and BRC-MFC) columns were constructed from nonopaque perspex. These columns were
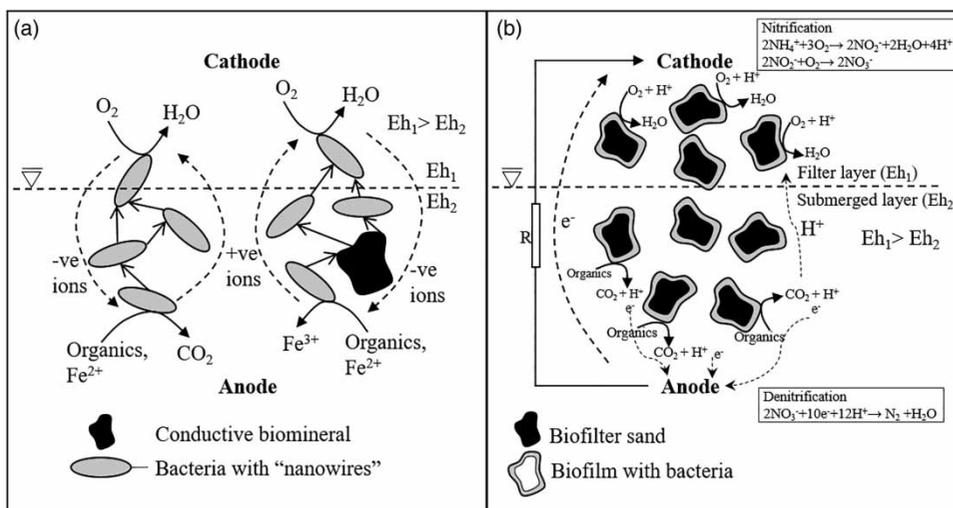

Figure 1 | Conceptual models of redox-associated mechanisms: (a) classical biogeobattery model*; (b) BRC-MFC model (*Revil *et al.* 2015).

fabricated using an acrylic column (8 cm depth × 70 cm height). Figure 2 shows the schematic diagram of BRC and BRC-MFC. These columns were located indoors at an average temperature of 30 ± 4°. The composition of bioretention media layers for saturated designs follow the Australian FAWB adoption guidelines (Payne et al. 2014b): a filter layer of washed sand (300 mm, diameter 0.15–1.00 mm), a transition layer of coarse sand (100 mm, diameter 0.50–1.00 mm), a sand submerged layer (200 mm, diameter 0.25–0.50 mm), and the bottom gravel drainage layer (100 mm, diameter 3–5 mm). Three columns with an elevated outlet provided a saturated zone in the lower half of the column ('saturated' design). These columns included a supplementary carbon source of pine chips comprising approximately 5% by volume of saturated zone.

The electrodes (anode and cathodes) employed in the current study were made of activated carbon. Activated carbon is a common carbon material used in the water treatment process. The high specific surface makes it a good medium for the attachment of microorganisms and characteristics of activated carbon such as good biocompatibility as well as moderate electrical conductivity make it a promising biocathode material (Yu et al. 2017). Activated carbon is one of the common materials in sewage treatment that has low resistivity $3.2 \times 10^6 \, \Omega cm$, high specific area

796 m^2/g and a high C/O mass ratio of 15.2. Activated carbon was immersed in the mixed cultivated sludge and fed with synthetic wastewater. The activated carbon reached saturation during the inoculation period, and acts as a medium for attachment of microbes for biological activity during operation. Thus, the virgin activated carbon transformed into biological activated carbon. Meanwhile, the activated carbon was only placed in the cathode and anode area, and its dosage was very little relative to the whole packing layer. Therefore, although the activated carbon may have an effect on the removal of nitrogen and phosphorus, its interference was negligible in the current experiment. The volume for each layer of anode and cathode electrode was 251.20 cm^3. Insulated copper wire was used to connect both the anode and cathode with an external resistance of 1,000 Ω to complete the circuit.

In order to create an anaerobic condition for the anodic region, the anode was positioned at 15 cm from the bottom of the column. Besides that, an elevated outlet was located for providing a saturated zone in the lower half of the column. The cathode was situated at 60 cm from the bottom of the column, complying with the aerobic condition. Three columns were kept unplanted in order to only assess the influence of different carbon nitrogen ratios and different combinations on nitrogen removal performance.
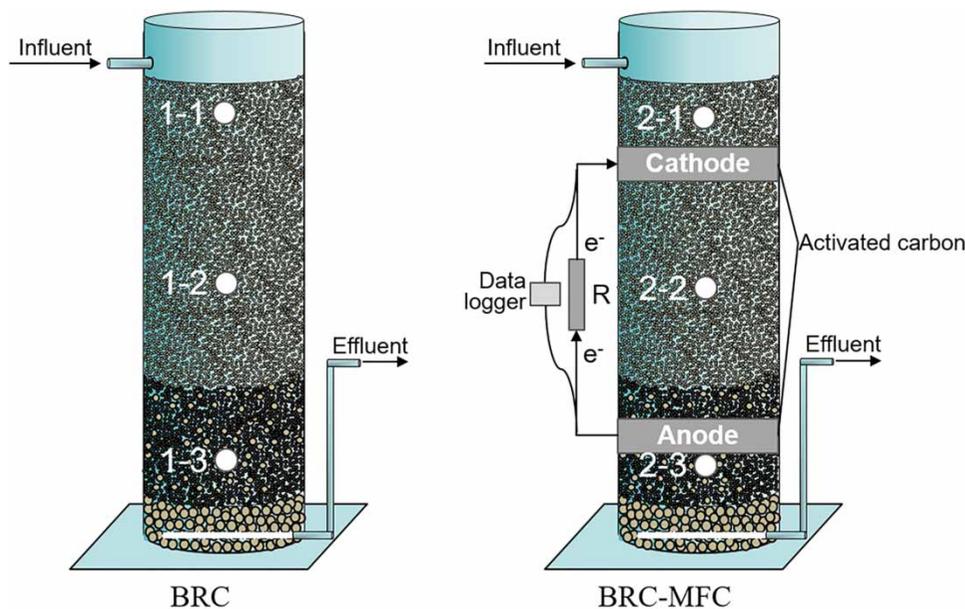

Figure 2 │ Schematic diagram of bioretention cell.

Synthetic wastewater

A synthetic wastewater containing the desirable amount of glucose as a carbon source was used throughout the study. The concentrations were targeted to typical domestic wastewater nutrient levels (concentration in g/L): varying amounts of $C_6H_{12}O_6$ (0.15 ± 0.003, 0.24 ± 0.02, 0.48 ± 0.01, 0.6 ± 0.005, and 1.2 ± 0.01); NH_4Cl (22.24 ± 0.03); K_2HPO_4 (2.18 ± 0.05); $NaHCO_3$ (8.73 ± 0.04); $FeCl_2 \cdot 4H_2O$ (4.82 ± 0.05); $CoCl_2 \cdot 6H_2O$ (0.39 ± 0.01); $NiCl_2 \cdot 6H_2O$ (0.19 ± 0.007); $MnCl_2 \cdot 4H_2O$ (0.01 ± 0.001); $CuSO_4$ (0.01 ± 0.001); $ZnCl_2$ (0.01 ± 0.001); $CaCl_2$ (0.04 ± 0.002); Humic acid (0.12 ± 0.005). All the chemical reagents used in this study were of analytical reagent (AR) grade (Wang *et al.* 2013).

Inoculation

Inoculation medium in the submerged layer and activated carbon were immersed in the mixed cultivated sludge for inoculation for 45 days, which was obtained from an anaerobic reactor in the local wastewater treatment plant (Nanjing Banqiao Water Group, Nanjing, China). During the inoculation period, synthetic wastewater was fed to the anaerobic inoculation tank to support the growth of the microbial community.

Experimental procedure

Synthetic wastewater was supplied to the top of the bioretention using a peristaltic pump (Longer BT100-2 J, China) at a flow rate of 3.5 mL/min (1.0 m^3/m^2 s hydraulic load (HLR)), operated in intermittent mode, which was maintained at 12 hours hydraulic retention time (HRT). Treated wastewater was discharged and collected from an elevated outlet.

The experiment was divided into five stages (over a total of 112 days): (1) Stage I, $C/N = 2:1$; (2) Stage II, $C/N = 4:1$; (3) Stage III, $C/N = 8:1$; (4) Stage IV, $C/N = 10:1$; (5) Stage V, $C/N = 20:1$. Experiments were conducted in triplicate with three treatment cells. Nitrogen and carbon levels under various C/N ratios were analyzed and compared.

Sample collection and determination

Influent and effluent of the experimental cells were sampled to evaluate transformation and treatment performance three times during each stage. The samples were immediately transported and analyzed at the Laboratory of Southeast University-Monash University Joint Research Centre. Chemical oxygen demand (COD) was determined with a HACH DR2800 (HACH Co., USA). Total nitrogen (TN), NH_4^+-N, NO_3^--N, and NO_2^--N were measured using a spectrophotometer UV-1800 (SHIMADZU Co., Kyoto, Japan), and total phosphorus (TP) was determined by the ammonium molybdate spectrophotometry method. All the parameters mentioned above were determined using the methods and procedures described in the Standard Method for Examination of Water and Wastewater (MoEE China 2002).

Microorganism samples were collected from submerged layers at the end of 150 days. For this sampling, three microorganism samples were taken from each column. After on-site collection, the samples were transported immediately to the laboratory for the purpose of total DNA extraction. The genomic DNA was extracted and purified using a MOBIO PowerSoil® DNA Isolation Kit (12888-50 Soil DNA Kit MOBIO, USA). The extracted genomic DNA was kept at −20° and detected using 1% agarose gel electrophoresis.

Data analysis

Influent and effluent concentrations were used to calculate the removal efficiencies and transformation or accumulation rates of COD, TN, NH_4^+-N, NO_2^--N, and NO_3^--N. Stepwise regression models were built to determine the multiple linear regression equation between nitrogen transformation rates and functional genes using SPSS Statistics 20 (IBM, USA). All data were analyzed using analysis of variance (ANOVA). Data were checked to ensure ANOVA assumptions were not violated and were transformed appropriately when needed prior to analysis.

RESULTS AND DISCUSSION

Effect of influent C/N ratio on COD removal

The trends of COD concentration and removal efficiency under different C/N operating conditions are presented in

Figure 3. The results revealed that when the influent C/N ratio fluctuates between 2.54 and 4.16, the average COD concentration of effluent from BRC group and BRC-MFC group was 24–42 and 17–27 mg/L, respectively. The average COD removal rates of BRC group and BRC-MFC group were 69.86 and 83.04% (C/N = 2.54); 79.82 and 92.04% (C/N = 4.16); 80.89 and 95.27% (C/N = 7.90); 80.26 and 97.63% (C/N = 10.42); 82.94 and 95.55% (C/N = 19.36), respectively.

It was noted in an earlier study that that the effective utilization rate of COD was 74% (C/N < 5.0) in the intermittent system (Cao *et al.* 2013). In contrast, the BRC-MFC enhanced group has obvious advantages in enhancing the utilization of carbon sources when treating wastewater with low C/N ratio under the same conditions. This is probably due to the fact that in the anode (anaerobic submerged layer), organic compounds are almost completely oxidized by microorganisms (Oon *et al.* 2016). Liu *et al.* (2019) determined that the COD removal rate of vertical flow constructed wetland coupled with MFC system was only 79.65% (about 505 mg/L of influent COD). In the current study, the COD removal rate was 95.27% (about 500 mg/L of influent COD) higher than previous research results. At

the same time, activated carbon functional groups will enhance the attachment of microorganisms on the surface of activated carbon (Wong *et al.* 2018). In addition, a closed loop was formed in the BRC-MFC strengthening system, which enhanced the electron transfer from the anode to the cathode and further affected the biodegradability of organic pollutants. Zhang *et al.* (2016) also found that the performance of constructed wetland coupled MFC system was 12–20% better than that of an open-circuit system, and 27–49% better than that of an ordinary constructed wetland without MFC. Therefore, this study indicates that the BRC-MFC system has a significant impact in organic degradation.

Effect of influent C/N ratio on nitrogen removal

As shown in Figure 4, NH_4^+-N and TN removal rates are closely related, mainly because the nitrification process provides an electron acceptor for denitrification. Complete oxidation of NH_4^+-N is the basis for effective TN removal. The average removal efficiencies of NH_4^+-N were 32.19% (BRC) and 42.26% (BRC-MFC) under C/N = 2.54. In terms of average removal efficiency of TN, the BRC-MFC
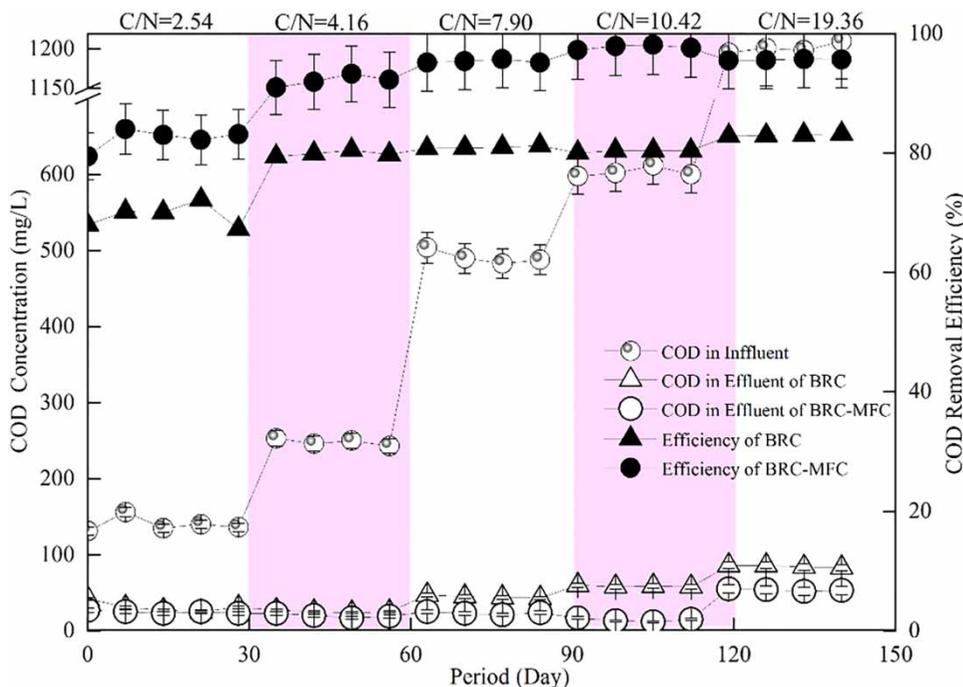
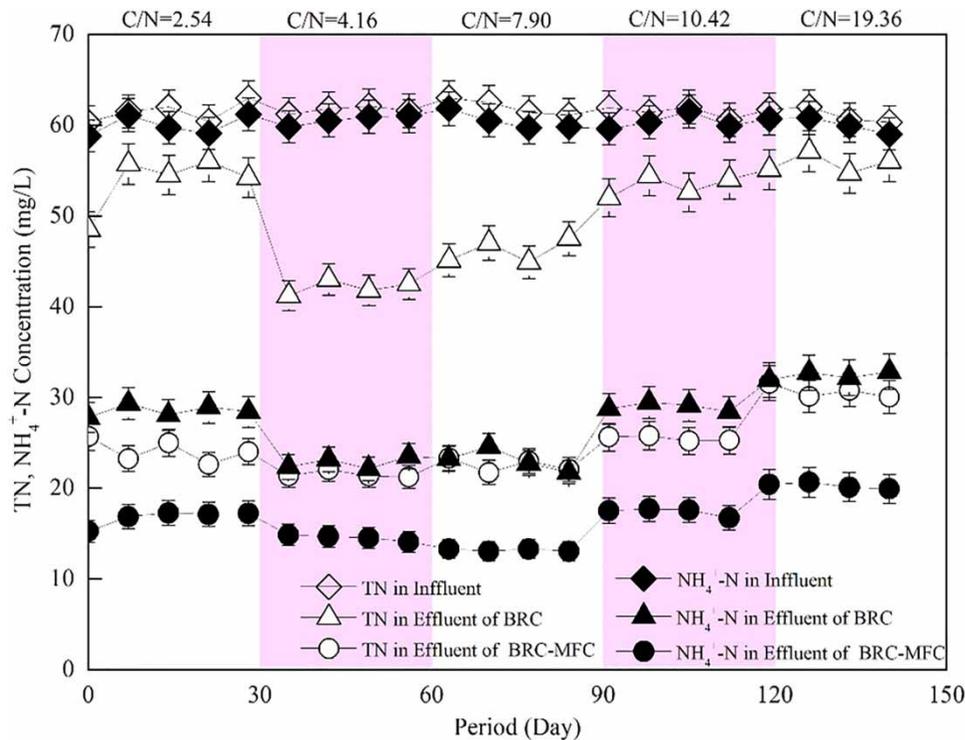**Figure 3** │ Removal performance of COD at different C/N ratios.

Figure 4 | Removal performance of TN and NH$_4^+$-N at different C/N ratios.

system (60.75%) was 75% higher than that of the BRC system. The average removal efficiency of TN and NH$_4^+$-N was significantly higher than that of other C/N ratios except for 4.16 and 7.90. The removal rates of TN and NH$_4^+$-N were hardly improved further, mainly because the cathode was located 10 cm below the top of the reaction column, which limits the electron acceptor (oxygen) and slows down the metabolism of nitrifying bacteria (Shen et al. 2018).

The results reveal that when the C/N ratio was increased to 10.42, the nitrification was intensified, and NH$_4^+$-N concentrations in the effluent of the BRC system and the BRC-MFC system gradually accumulated, reaching 46.22 and 28.86 mg/L, respectively. The average TN removal rates were 24.41 and 52.80%, respectively. Combined with the utilization of COD, the decrease in nitrogen removal efficiency was mainly due to the incomplete nitrification caused by the excessive loading of influent organic matter, resulting in the decrease of TN removal rate. The removal rates of TN and NH$_4^+$-N were difficult to further improve, mainly because the cathode was located 10 cm below the top of the column, which limits

the electron acceptor (oxygen) and then slows down the metabolism of nitrifying bacteria.

The above results reveal that, in a certain range, improving the influent C/N was an effective measure to improve the TN removal efficiency, but this must be based on the complete oxidation of NH$_4^+$-N, otherwise the excessive C/N will not only cause the waste of carbon sources, but also lead to the deterioration of nitrogen removal. Figure 5 shows the trend of NO$_3^-$-N and NO$_2^-$-N changing with different C/N. As shown in Figure 5, the high plateau of the NO$_3^-$-N concentration curve was observed in the BRC system under C/N = 2.54, and because of insufficient demand for denitrifying organic matter, it is more advantageous to produce nitrite from ammonia than from nitrate. A possible reason could be that low C/N influent cannot meet the organic matter required for denitrification, which also leads to the accumulation of NO$_3^-$-N.

In the BRC-MFC system with influent C/N of 4.16, NO$_2^-$-N accumulated significantly, but NO$_3^-$-N did not accumulate. The possible reason was that COD decreased and the supply of electron donors was insufficient. This trend is consistent with the findings of Wu et al. (2009),
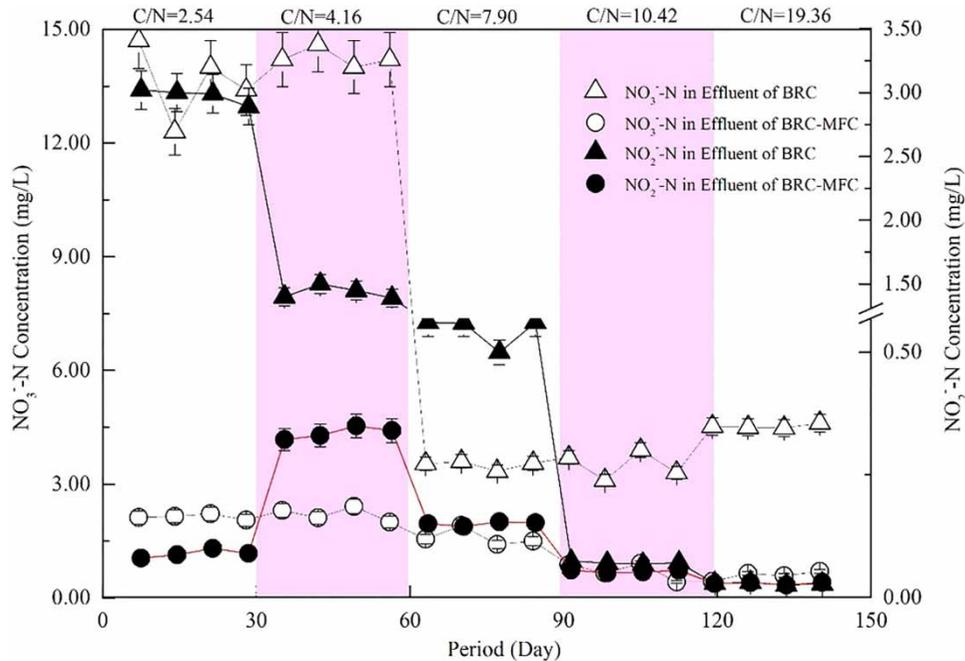
Figure 5 | Removal performance of NO_3^--N and NO_2^--N at different C/N ratios.

where they noted that NO_2^--N increases during denitrification when the supply of electron donors was insufficient. When influent C/N was 10.42 and 19.36, the concentration of NO_3^--N decreases (Figure 5), and the concentration of NO_3^--N increases gradually (Figure 4). The possible reason could be that the nitrate was changed by dissimilatory nitrate reduction to ammonium (DRNA) process, and DRNA dominates the reduction of NO_3^- and NO_2^- in anoxic environments. This process is in competition with denitrification, especially under high influent C/N conditions (Xu et al. 2017). The average voltage of BRC-MFC system reaches 35.5 mV, and the maximum power density was 103.83 mW/m³. Hence, it could be concluded that under the electric enhancement condition, the electron migration in the system is beneficial to denitrification and improves the overall nitrogen removal performance.

Effect of different C/N ratio and C/P ratio on simultaneous removal of nitrogen and phosphorus

The results showed that the change of influent C/N had little effect on the removal of COD and TP, but the simultaneous removal of nitrogen and phosphorus was based on

sufficient electron acceptor, BRC-MFC system had obvious advantages in enhancing the utilization of carbon sources and the ability of electron transfer under low influent C/N. Therefore, the correlations between the value of C/N and C/P and the removal rate of TN and TP were compared.

As shown in Figure 6, when C/N < 3 or C/P < 40, the TN and TP removal rates of BRC were less than 20 and 70%, respectively. The TN removal rate of BRC-MFC was lower than 60%, and the TP removal rate was about 97%. In C/N > 4 or C/P > 60 conditions, the TN removal rates of both systems revealed a downward trend, and TP removal rates were basically stable. This trend is consistent with the earlier findings (Xu et al. 2019). Therefore, under C/N = 3–4 or C/P = 30–60 conditions, the removal rates of TN and TP in BRC system were 33 and 75%, respectively, and the treatment efficiency was limited. The removal rates of TN and TP in BRC-MFC system reached 65 and 98%, respectively, which basically realized the simultaneous removal of nitrogen and phosphorus. Meanwhile, the removal efficiency of the BRC system was improved by 30%.

Although the average voltage and maximum power density were not as good compared to the findings of Xu et al. (2018) in the CW-MFC (the average voltage was
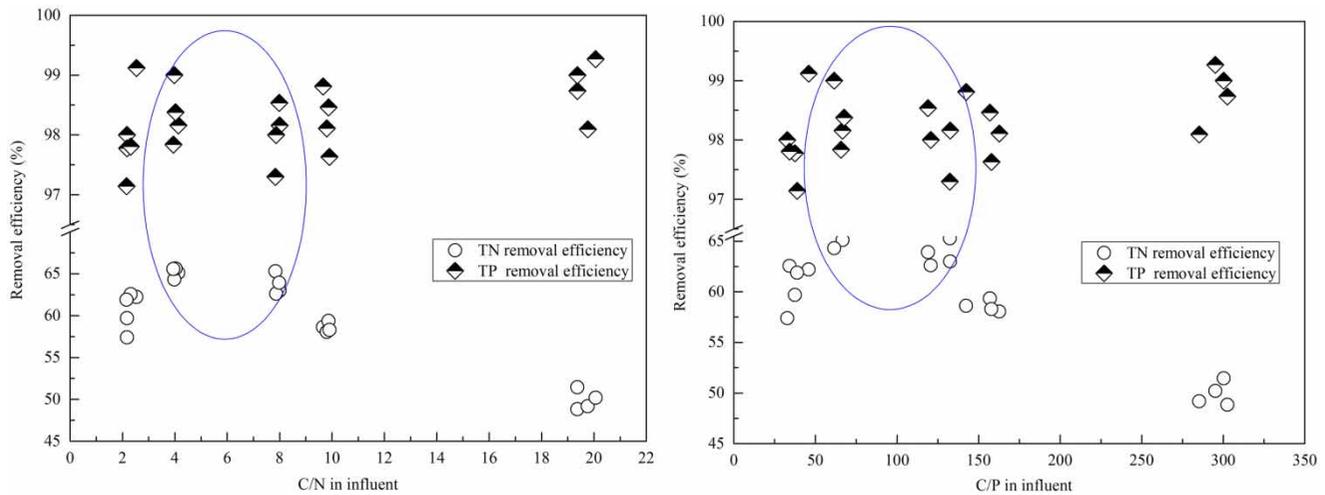
Figure 6 │ Correlations of TN and TP removals with influent C/N and C/P ratios.

265.77 ± 12.66 mV and the highest power density was $3,714.08$ mW/m^2), the removal rate of all pollutants by BRC-MFC in the current study was higher than that by CW-MFC. Under different electric enhancement conditions, the electron migration in the system was beneficial to denitrification and improves the overall nitrogen removal performance.

Comparative study on permeation characteristics of MFC strengthened group and BRC control group

The BRC-MFC system and the BRC system were tested for sewage infiltration with 1.0 m^3/(m$^2 \cdot$d) hydraulic load (porosity $= 41\%$, initial permeability coefficient $K_{ini} = 3.893 \times 10^{-4}$ m/s, influent C/N $= 4$, inlet/reaction time $= 1/8$, intermittent operation cycle), the results are presented in Figure 7. As shown in Figure 7, the standard permeability coefficient K_{20} of BRC-MFC and BRC systems decreases with the running time, but the changing process was different. The BRC system has experienced the three following stages: the permeability coefficient of the first stage (0–57 d) dropped sharply (slope $K_{2-1} = -0.0416$); decreased slowly in the second stage (59–121 d) (slope $K_{2-2} = -0.0055$); but reached a more stable state in the third stage on the 123rd day, where K_{20} (BRC) reduced to 0.89×10^{-4} m/s (accounting for 23% of K_{ini}).

In contrast, the BRC-MFC system experienced four stages, the permeability coefficient of the first stage

(0–25 d) system dropped sharply (slope $K_{1-1} = -0.0332$). The slope for the BRC system is slightly lower than the BRC-MFC system and revealed low permeability coefficient values in the BRC system. The reason could be that the structure and diversity of microbial community in the filler layer were changed by the increase of electron transport. *Proteobacteria* (31%), *Bacteroidetes* (21%) and *Chloroflexi* (14%) were the dominant bacteria in the BRC-MFC system, while the dominant bacteria in the BRC system were mainly *Chlorobi* (45%) and *Proteobacteria* (21%). The second stage (27–49 d) appeared to be a plateau stage, mainly because MFC enhanced the ability of microorganisms to degrade pollutants, and the microbial biomass could be evenly distributed throughout the reaction column region, thus making the permeability more stable. In the third stage (51–111 d), the permeability coefficient of the system continued to decline again. A possible reason could be the coupling effect of multiple influencing factors. The accumulation of inorganic/organic compounds and the growth of biofilm would inevitably lead to the gradual decrease of the pore space in the reaction column, and consequently the permeability coefficient gradually decreased.

Although the decrease was greater than that of the second stage of BRC (slope $K_{1-3} = 0.0102 > K_{2-2} = 0.0055$), compared to the BRC system, BRC-MFC reached the stable platform 10 days ahead of schedule, the K_{20} (BRC-MFC) was reduced to 1.86×10^{-4} m/s (48% of K_{ini}), which was
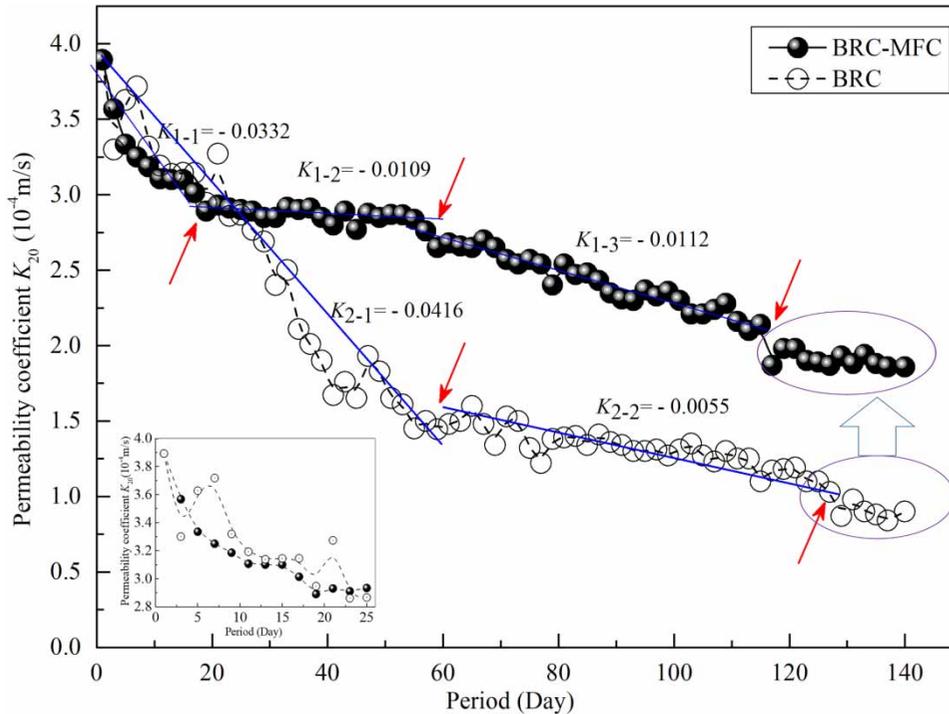
Figure 7 │ Trend of the permeability coefficient of BRC and BRC-MFC.

twice that of the BRC system in the stable stage. Therefore, the BRC-MFC system can delay the 50% reduction of permeability coefficient, and can enter the stable stage of permeability coefficient earlier.

In a previous study about the BRC treatment (Coustumer *et al.* 2009), the removal rate of TN decreases with the decrease of permeability coefficient. The highest removal rate of TN (51%) occurs in the middle region of the permeability coefficient. Similar changes were also found in the current study. The difference is that the highest TN removal rate occurred in the low permeability area. This trend is different from the previous study (Coustumer *et al.* 2009). BRC-MFC can not only delay the decrease of permeability coefficient, but also enhance the TN removal efficiency. Therefore, BRC-MFC has the effect of simultaneous denitrification and stable permeability.

Biomass distribution on the sand of differential reactors

The biofilm samples were analyzed on the 90th and 150th day of the experiment by opening a BRC column as a control group and a BRC-MFC column, and then different locations

were collected from the top (filter layer), the middle (submerged layer) and the bottom (drainage layer) and directly observed by Confocal Laser Scanning Microscope (CLSM), as shown in Figure 8.

As shown in Figure 8 and Table 1, the distribution of biofilm on the sand surface of the two systems shows an increasing trend with time. However, the growth/decrease in biofilm thickness and its spatial distribution in each system were different. Compared to BRC system, the biofilm thickness of BRC-MFC system was 2-3 > 2-2 > 2-1, but the values were basically close. As microorganisms catalyze substrate denitrification by respiration to produce electrons, electrodes act as temporary electron acceptors to absorb electrons and transfer electrons to the cathode surface through a loop for pollutant degradation in the cathode region. Thus nutrients can be effectively degraded and removed when they firstly contact the 2-1 region (upper filter layer). At the same time, the microbial community in the 3-1 sampling site was in the unsaturated filter layer, without sufficient HRT and long-term mass transfer of nutrients. On the contrary, the 2-2 and 2-3 regions were saturated (with submerged area) which could ensure the contact
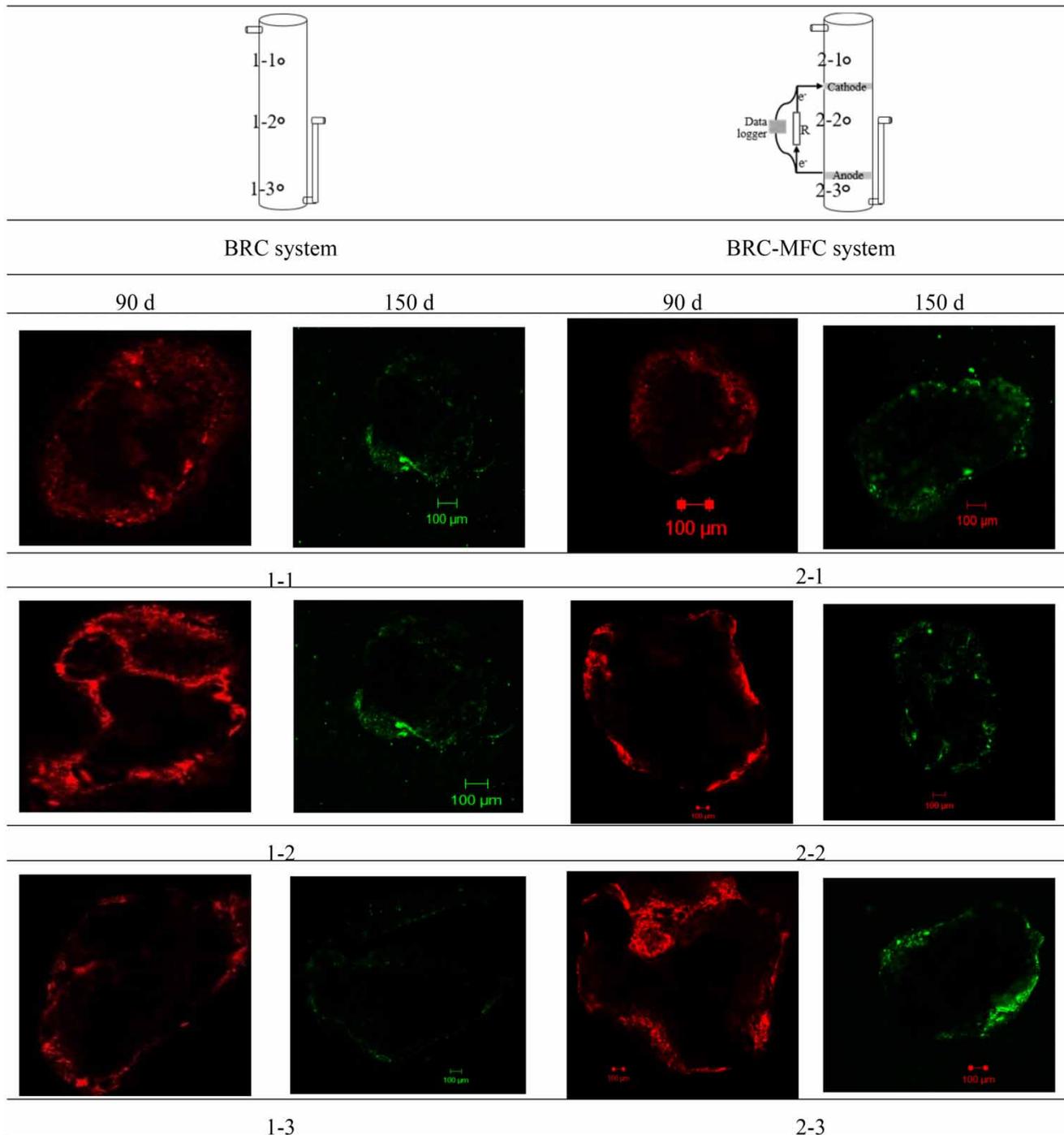
Figure 8 | Biomass distribution on the sand of differential reactors.

adsorption and degradation of microorganisms and nutrients, and promote microbial growth. Compared with the BRC system, the BRC-MFC system had a considerable increase in the thickness of biofilm and the proportion of sand surface area, and formed a uniform 'upper thin and lower thick' spatial distribution, which enhanced the ability to resist the accumulation of pollutants on the surface of the reaction system.

Table 1 | Thickness of biofilm on sand after 90 and 150 day inoculations

Sampling location	Time (days)	Biofilm thickness range (μm)	Biofilm thickness (μm)	Biofilm specific surface ratio (%)
1–1	90	0–75	36.5	80
	150	0–80	38.0	85
1–2	90	0–85	55.1	87
	150	15–120	57.2	95
1–3	90	0–60	25.5	68
	150	5–65	31.0	75
2–1	90	0–100	55.0	90
	150	0–95	75.3	95
2–2	90	0–200	102.5	95
	150	31–190	90.3	100
2–3	90	23–150	82.0	100
	150	41–186	94.0	100

Phylogenetic diversity of bacterial communities

Many scholars have proved that *Proteobacteria*, *Firmicutes*, *Acidobacteria* and *Bacteroidetes* have electrochemical activity (Lee *et al.* 2003), *Citrobacter* (Chen *et al.* 2017) and *Geobacter* of *Proteobacteria* and *Clostridium* were the dominant bacteria producing electricity. All of these were found to exist in the BRC-MFC system. As shown in Tables 2 and 3, the relative abundance of *Proteobacteria* and *Bacteroidets* in the BRC-MFC system increased gradually with time, and by the 200th day, the relative abundance was 41 and 13%, respectively. The relative abundance of *Dok59* and *Geobacter* was high in all bacteria (9 and 6%, respectively). It indicates that the electricity producing bacteria group is not limited to the *Geobacter* bacteria. Therefore, the discovery of electro bacterium *Dok59* has expanded the scope of electro-generated microorganisms. The difference in the microbial community structure may be due to the composition of the fuel cell packed with sediment and its degradation products (Dong *et al.* 2017). In the BRC system, the *Rhodanobacter* content was relatively stable over time, with a content of 3%. It can be concluded that the composition and structure of the microbial community in the system did not change significantly without the intervention of bioelectric intensification, and anaerobic denitrifying bacteria were the dominant species.

Practical applications and future research perspectives

Current research findings provide a technical guideline to enhance the long term operation reliability and denitrification performance of BRC systems for an intermittent domestic sewage treatment in China and other developing countries.

Table 2 | Relative abundance distribution of bacterial species in experimental group (unit: %)

	BRC system		BRC-MFC system	
	(90 d)	(200 d)	(90 d)	(200 d)
Top ten	*Chlorobi*, 45	*Proteobacteria*, 40	*Proteobacteria*, 31	*Proteobacteria*, 41
	Proteobacteria, 21	*Bacteroidetes*, 21	*Bacteroidetes*, 21	*Chloroflexi*, 18
	Chloroflexi, 10	*Chloroflexi*, 9	*Chloroflexi*, 14	*Bacteroidetes*, 13
	Bacteroidetes, 8	*Chlorobi*, 4	*Fibrobacteres*, 11	OD1, 7
	Spirochaetes, 4	OD1, 4	*Chlorobi*, 10	*Chlorobi*, 5
	Firmicutes, 3	*Acidobacteria*, 3	*Spirochaetes*, 4	*Fibrobacteres*, 2
	Acidobacteria, 2	*Firmicutes*, 3	*Acidobacteria*, 1	*Nitrospirae*, 2
	WS6, 1	*Verrucomicrobia*, 3	*Firmicutes*, 1	OP11, 2
	Verrucomicrobia, 1	*Chlamydiae*, 2	*Verrucomicrobia*, 1	*Acidobacteria*, 1
	OD1, 1	*Cyanobacteria*, 2	OD1, 1	*Actinobacteria*, 1
Other	*Nitrospirae*	*Spirochaetes*, 2	*Candidate division*, WS6, TM7	*Cyanobacteria*
	Cyanobacteria	*Actinobacteria*	*Cyanobacteria*	*Firmicutes*
	TM7	*Planctomycetes*	*Nitrospirae*	*Planctomycetes*
		Fibrobacteres		*Spirochaetes*
		Gemmatimonadetes		*Verrucomicrobia*
		Nitrospirae		*Chlamydiae*
		OP11, TM6		*Gemmatimonadetes*
				TM6

Table 3 | Relative abundance distribution of bacterial genus in experimental group (unit: %)

	BRC system (200 d)	BRC-MFC system (200 d)
Top ten	Dok 59, 4	Dok 59, 9
	Rhodanobacter, 3	*Geobacter*, 6
	Chlorobaculum, 2	*Chlorobaculum*, 3
	Dechloromonas, 2	*Dechloromonas*, 2
	Simplicispira, 2	*Devosia*, 2
	Syntrophus, 2	*Anaerolinea*, 1
	T78, 2	*Thiobacillus*, 1
	Clostridium, 1	*Treponema*, 1
	Flavihumibacter, 1	*Uliginosibacterium*, 0.2
	Sediminibacterium, 1	*Syntrophus*, 0.2

In future research, the long-term running permeability coefficient change test under the clean water condition should be added, so as to make a comparative study with the results of the permeability coefficient change test under sewage conditions, so as to better reveal the change rule of BRC internal permeability coefficient. The future research should also carry out the operation of the BRC system under the real sewage conditions so that the findings could be beneficial in the actual field application environment.

CONCLUSIONS

The results showed that removal rates of TN and TP were 33 and 75%, respectively when the C/N ratio was 3–4 or the C/P ratio was 30–60 in BRC system, but the treatment efficiency was limited. The removal rates of TN and TP in BRC-MFC system reached 65 and 98%, respectively, with simultaneous removal of nitrogen and phosphorus. Permeability characteristics results showed that BRC-MFC system can delay the decrease of permeability coefficient by 50%, and can enter in the stable stage earlier. The BRC-MFC system has better stabilizing percolation performance and denitrification effects than the BRC system under long-term intermittent operation.

ACKNOWLEDGEMENTS

REFERENCES

Cao, G., Wang, S., Peng, Y. & Miao, Z. 2013 Biological nutrient removal by applying modified four step-feed technology to treat weak wastewater. *Bioresour. Technol.* **128** (1), 604–611.

Chen, C. Y., Tsai, T. H., Wu, P. S., Tsao, S. E., Huang, Y. S. & Chung, Y. C. 2017 Selection of electrogenic bacteria for microbial fuel cell in removing Victoria blue r from wastewater. *J. Environ. Sci. Health A* **53**, 1–8.

Coustumer, S. L., Fletcher, T. D., Deletic, A., Barraud, S. & Lewis, J. F. 2009 Hydraulic performance of biofilter systems for stormwater management: influences of design and operation. *J. Hydrol.* **376** (1), 16–23.

Dong, G. R., Kariminia, H. R., Chen, Z. W., Parker, W., Pritzker, M. D. & Legge, R. L. 2017 Enhancement of electricity generation by a microbial fuel cell using a highly active non-precious-metal nitrogen-doped carbon composite catalyst cathode. *Energy Fuels* **31** (1), 959–967.

Ge, Z., Wei, D., Zhang, J., Hu, J., Liu, Z. & Li, R. 2019 Natural pyrite to enhance simultaneous long-term nitrogen and phosphorus removal in constructed wetland: three years of pilot study. *Water Res.* **148**, 153–161.

Lee, J., Phung, N. T., Chang, I. S., Kim, B. H. & Sung, H. C. 2003 Use of acetate for enrichment of electrochemically active microorganisms and their 16 s rdna analyses. *FEMS Microbiol. Lett.* **223** (2), 185–191.

Liu, F., Sun, L., Wan, J., Tang, A., Deng, M. & Wu, R. 2019 Organic matter and ammonia removal by a novel integrated process of constructed wetland and microbial fuel cells. *RSC Adv.* **9** (10), 5384–5393.

Ministry of Ecology and Environment of the People's Republic of China 2002 *Standard Method for the Examination of Water and Wastewater*. Environmental Science Press of China, Beijing.

Oon, Y. L., Ong, S. A., Ho, L. N., Wong, Y. S., Dahalan, F. A., Oon, Y. S. & Thung, W. E. 2016 Synergistic effect of up-flow constructed wetland and microbial fuel cell for simultaneous wastewater treatment and energy recovery. *Bioresour. Technol.* **203**, 190–197.

Payne, E. G., Pham, T., Cook, P. L., Fletcher, T. D., Hatt, B. E. & Deletic, A. 2014a Biofilter design for effective nitrogen

removal from stormwater – influence of plant species, inflow hydrology and use of a saturated zone. *Water Sci. Technol.* **69** (6), 1312–1319.

Payne, E. G. I., Fletcher, T. D., Cook, P. L. M., Deletic, A. & Hatt, B. E. 2014b Processes and drivers of nitrogen removal in stormwater biofiltration. *Crit. Rev. Environ. Sci. Technol.* **44** (7), 796–846.

Revil, A., Mendonca, C. A., Atekwana, E. A., Kulessa, B., Hubbard, S. S. & Bohlen, K. J. 2015 Understanding biogeobatteries: where geophysics meets microbiology. *J. Geophys. Res. Biogeosci.* **115** (G1), 379–384.

Shen, X., Jian, Z., Liu, D., Zhen, H. & Liu, H. 2018 Enhance performance of microbial fuel cell coupled surface flow constructed wetland by using submerged plants and enclosed anodes. *Chem. Eng. J.* **351**, 312–318.

Wang, Q., Ye, L., Jiang, G. & Yuan, Z. 2013 A free nitrous acid (fna)-based technology for reducing sludge production. *Water Res.* **47** (11), 3663–3672.

Wong, S., Ngadi, N., Inuwa, I. M. & Hassan, O. 2018 Recent advances in applications of activated carbon from biowaste for wastewater treatment: a short review. *J. Clean. Prod.* **175**, 361–375.

Wu, J., Jian, Z., Jia, W., Xie, H., Gu, R. R., Cong, L. & Gao, B. 2009 Impact of COD/N ratio on nitrous oxide emission from microcosm wetlands and their performance in removing nitrogen from wastewater. *Bioresour. Technol.* **100** (12), 2910–2917.

Xu, D., Xiao, E., Xu, P., Lin, L., Zhou, Q., Xu, D. & Wu, Z. 2017 Bacterial community and nitrate removal by simultaneous heterotrophic and autotrophic denitrification in a bioelectrochemically-assisted constructed wetland. *Bioresour. Technol.* **245** (Pt A), 993–999.

Xu, F., Cao, F. Q., Kong, Q., Zhou, L. L., Yuan, Q., Zhu, Y. J., Wang, Q., Du, Y.-D. & Wang, Z.-D. 2018 Electricity production and evolution of microbial community in the constructed wetland-microbial fuel cell. *Chem. Eng. J.* **339**, 479–486.

Xu, R., Zhang, Y., Liu, R., Cao, Y., Wang, G., Ji, L. & Xu, J. 2019 Effects of different substrates on nitrogen and phosphorus removal in horizontal subsurface flow constructed wetlands. *Environ. Sci. Pollut. Res.* **2**, 1–10.

Yu, Y. Y., Zhai, D. D., Si, R. W., Sun, J. Z., Liu, X. & Yong, Y. C. 2017 Three-dimensional electrodes for high-performance bioelectrochemical systems. *Int. J. Mol. Sci.* **18** (1), 90–98.

Zhang, M., Peng, Y.-Z., Zhang, J.-H., Wang, C., Wang, S.-Y. & Zeng, W. 2016 Effect of influent C/N ratios on denitrifying phosphorus removal characteristics in the A2/O-BCO process. *China Environ. Sci.* **36** (5), 1366–1375.

Zhou, F., Cheng, S., Hui, W., Xian, C. & Li, X. 2017 Feasibility study of simultaneous azo dye decolorization and bioelectricity generation by microbial fuel cell-coupled constructed wetland: substrate effects. *RSC Adv.* **7** (27), 16542–16552.